

ONLINE SUPPLEMENTING MATERIAL FOR

APPLICATION OF AN ENSEMBLE EARTHQUAKE RATE MODEL IN ITALY, CONSIDERING EARTHQUAKE CATALOGS AND SEISMOGENIC SOURCES MOMENT RELEASE

Maura Murru^{*,1}, Giuseppe Falcone¹, Matteo Taroni¹ and Rodolfo Console^{1,2}

¹ Istituto Nazionale di Geofisica e Vulcanologia, Roma, Italy

² Center of Integrated Geomorphology for the Mediterranean Area, CGIAM, Potenza, Italy

(*) Corresponding Author: Maura Murru, Istituto Nazionale di Geofisica e Vulcanologia, Via di Vigna Murata, 605 - 00143 Rome – Italy (Fax: +39-06-51860507, Tel.: +39-06-51860412, maura.murru@ingv.it)

Contents of this file

Text S1 to S5

Figures S1 to S7

Table S1

Introduction

This supporting information provides for the time-independent model the results for three versions of the ensemble model (Ensemble 4, Ensemble 5, Ensemble 6) referring to the completeness time window determined from statistical approach (SAC). These versions assign different weights to the seismogenic sources and smoothed earthquake seismicity rate.

More information is given for the Italian Parametric Earthquake Catalog (CPTI15, release 1.5, Rovida et al. 2016, <http://emidius.mi.ingv.it/CPTI15-DBM15/>).

This Supporting Information also contains two Tables (S1a,b) referring to the Historical and Statistical Analysis of Completeness (HAC and SAC), respectively.

S1. The Italian Parametric Earthquake Catalog (CPTI15) – completeness time-windows

This section provides for the CPTI15 catalog, for the period 1000-2014, in a table format two different sets of completeness time windows depending on the magnitude intervals (regionally dependent).

These two different sets were determined from Historical and Statistical Analysis of Completeness (HAC and SAC), Table S1(a) and S1(b), respectively. The tables of completeness were provided by the authors of the CPTI15 catalog in the framework of the new Italian seismic hazard map (Meletti *et al.* 2018). More details can be found in Albini *et al.* (2001), Albini *et al.* (2002) and Albarello *et al.* (2001). The reader can also refer to:

https://emidius.mi.ingv.it/CPTI15-DBMI15/description_CPTI15_en.htm

The definition of the completeness intervals is provided on the basis of a breakdown of magnitude bin (Table S1(a) and S1(b), respectively). Five Italian macro-areas (Alps, Po Plain, Center, South, Islands, including both Sardinia and Sicily, with red polygons in Fig. S1) are considered homogeneous for spatial and temporal completeness. In addition, another zone defined as “Outside”, number 6, is considered as the zone outside the others. It includes all events that do not fall within the five macro-areas but are still within the target area (black line in Fig. S1). Fig. S1 displays in space the shallow earthquake declustered catalog, falling inside time periods of completeness of each macro-areas, shown in Table S1 (a).

Table S1. The table contains the minimum bound of the time window of completeness for **(a)** Historical and **(b)** Statistical approaches in years (A.D.) for the six Italian macro-areas (numbers refer to Fig. S1). The column “Islands” refers to both Sicily and Sardinia.

(a)

M_w min	M_w	M_w max	M_w bin	Alps (1)	Po Plain (2)	Center (3)	South (4)	Islands (5)	Outside (6)
3.845	3.96	4.075	1	1900	1950	1950	1950	1950	2002
4.075	4.19	4.305	2	1900	1836	1900	1895	1950	2002
4.305	4.42	4.535	3	1871	1836	1871	1895	1871	2002
4.535	4.65	4.765	4	1871	1836	1871	1895	1871	1984
4.765	4.88	4.995	5	1871	1836	1871	1895	1871	1984
4.995	5.11	5.225	6	1700	1530	1650	1787	1700	1984
5.225	5.34	5.455	7	1700	1530	1650	1787	1700	1984
5.455	5.57	5.685	8	1530	1530	1650	1787	1700	1963
5.685	5.80	5.915	9	1530	1300	1530	1787	1530	1963
5.915	6.03	6.145	10	1300	1300	1530	1530	1530	1963
6.145	6.26	6.375	11	1300	1100	1300	1530	1300	1963
6.375	6.49	6.605	12	1300	1100	1300	1400	1300	1963
6.605	6.72	6.835	13	1300	1100	1300	1400	1300	1963
6.835	6.95	7.065	14	1300	1100	1300	1400	1300	1963
7.065	7.18	7.295	15	1300	1100	1300	1400	1300	1963
7.295	7.41	7.525	16	1300	1100	1300	1400	1300	1963

(b)

M_w min	M_w	M_w max	M_w bin	Alps (1)	Po Plain (2)	Center (3)	South (4)	Islands (5)	Outside (6)
3.615	3.73	3.845	0	1870	1870	1880	1960	1890	1960

3.845	3.96	4.075	1	1870	1870	1880	1960	1890	1960
4.075	4.19	4.305	2	1870	1870	1880	1960	1890	1960
4.305	4.42	4.535	3	1870	1870	1880	1960	1890	1960
4.535	4.65	4.765	4	1850	1870	1880	1870	1870	1960
4.765	4.88	4.995	5	1850	1870	1880	1870	1870	1960
4.995	5.11	5.225	6	1810	1830	1790	1820	1680	1930
5.225	5.34	5.455	7	1810	1830	1790	1820	1680	1930
5.455	5.57	5.685	8	1530	1690	1750	1760	1600	1930
5.685	5.80	5.915	9	1530	1690	1750	1760	1600	1930
5.915	6.03	6.145	10	1490	1450	1580	1660	1500	1930
6.145	6.26	6.375	11	1490	1450	1580	1660	1500	1930
6.375	6.49	6.605	12	1490	1320	1580	1600	1500	1930
6.605	6.72	6.835	13	1490	1320	1580	1600	1500	1930
6.835	6.95	7.065	14	1490	1320	1580	1550	1500	1930
7.065	7.18	7.295	15	1490	1320	1580	1550	1500	1930
7.295	7.41	7.525	16	1490	1320	1580	1550	1500	1930

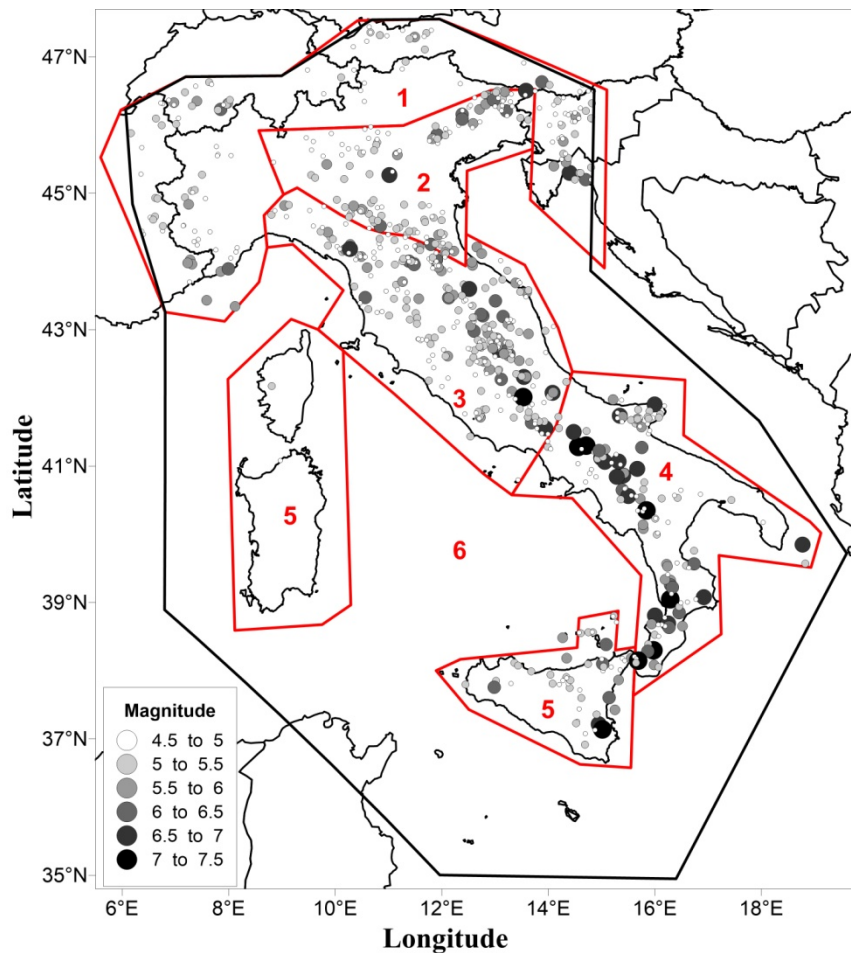


Figure S1. Map displaying the CPTI15 catalog in space, as well as the macro-areas considered homogeneous in terms of completeness. Only the earthquakes falling inside time periods of completeness (HAC) are shown, colored in grey scale according to the magnitude size. The black polygon shows the area under analysis, called the “areaCPTI15”. The red polygons and numbers refer to the Italian macro-areas of the CPTI15 catalog (Table S1).

S2. Seismic catalog considering Statistical Analysis of the Completeness (SAC)

This part refers to the shallow catalog that includes the events of the CPTI15 selected by the Statistical Analysis of the Completeness (SAC), for the period 1000-1980, and the Instrumental catalog (1981-April 30, 2017, from M_w 3.0). Fig. S2 shows the declustered seismicity distribution of this dataset, named through the manuscript with the acronym *CAT_S*.

The CPTI15 is shown with blue and black colors (blue dots and black squares indicate earthquakes from M_w 3.845+ and from M_w 5.5+, respectively). The Instrumental Catalog (1981-April 30, 2017) (M_w 3.0+ and depth ≤ 30 km) is indicated with green and red colors (green dots and red squares indicate earthquakes from M_w 3.0+ and from M_w 5.5+, respectively). The black polygon shows the investigated area, called the “areaCPTI15”.

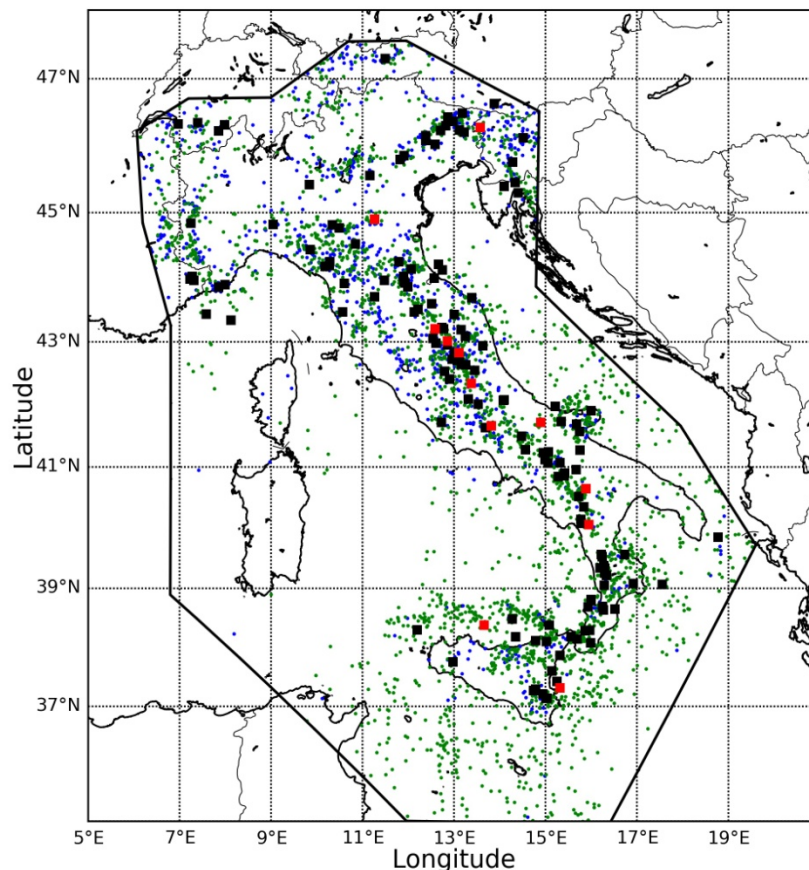


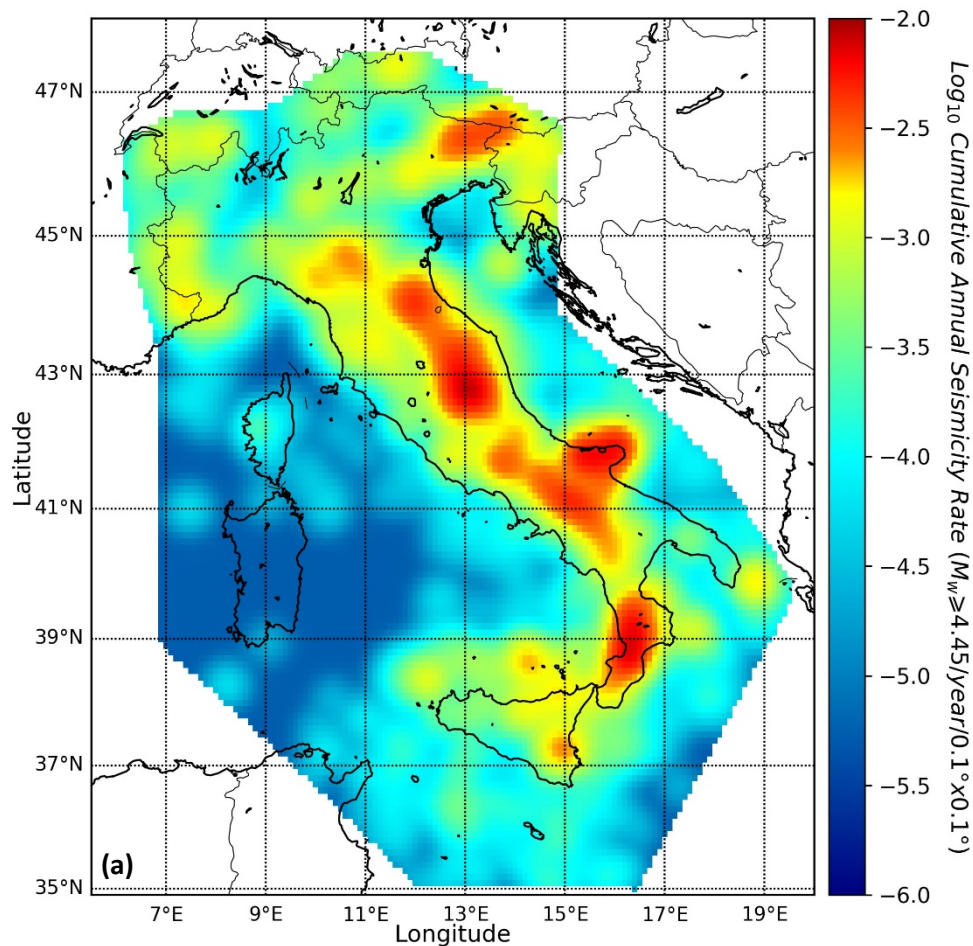
Figure S2. Seismicity map obtained by combining the declustered CPTI15 and Instrumental Catalogs. In this selection of seismic data, the *CAT_S* catalog was considered.

The CPTI15 is shown with blue and black colors (blue dots and black squares indicate earthquakes from $M_w \geq 3.845$ and from $M_w \geq 5.5$, respectively). The Instrumental Catalog (1981-April 30, 2017)

(M_w 3.0+ and depth ≤ 30 km) is indicated with green and red colors (green dots and red squares indicate earthquakes from $M_w \geq 3.0$ and from $M_w \geq 5.5$, respectively). The black polygon shows the investigated area, called the “areaCPTI15”.

S3. Smoothed seismicity

Figs. S3(a) and (b) show the smoothed spatial seismicity with completeness magnitude correction (Hiemer *et al.* 2014) for the catalog described in the previous section. Two scales were considered to show the results: logarithmic and linear. The correlation distance obtained for this dataset is equal to 23 km.



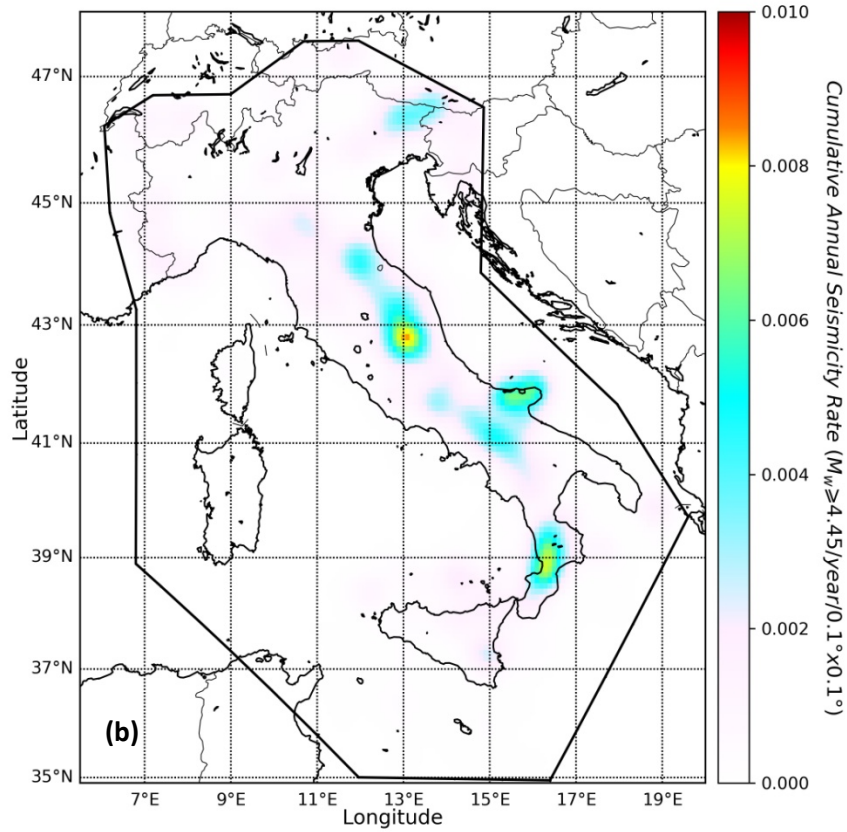


Figure S3. Smoothed distribution for the declustered seismicity (1000-April 2017) that includes the *CAT_S* catalog . The correlation distance obtained for this dataset is equal to 23 km. The color scale represents the \log_{10} annual cumulative seismicity rate for $M_w \geq 4.45$ in cells of $0.1^\circ \times 0.1^\circ$. **(a)** Results on a logarithmic scale. **(b)** Results on a linear scale.

The resulting cumulative annual rate of events for the smoothed seismicity model, inside the entire area studied, $M_w \geq 4.45$, in cells of $0.1^\circ \times 0.1^\circ$, is 6.02 for SAC compared to 5.68 for HAC .

The b-value and the corner magnitude estimated using this catalog are 0.99 and M_w 7.3, respectively (the same values obtained using the HAC).

S4. Development of the integral calculation for the seismic moment released by earthquakes

In the main text (subsection 3.2) we have dealt with the determination of the annual rates from the Database of the Italian Seismogenic Sources version 3.2.1 (DISS Working Group 2018). To obtain them, we need to estimate the total seismic moment of each seismogenic source, M , released by earthquakes. The expected value is derived from the following formula:

$$\int_{M_t}^{inf} \left(M \frac{dF(M)}{dM} \right) dM$$

(S1)

where $\frac{dF(M)}{dM}$ is the Probability Density Function and M_t is the threshold seismic moment for completeness. The cumulative distribution function (CDF) $F(M)$ is the tapered *Gutenberg-Richter* (TGR) relation:

$$F(M) = 1 - \left(\frac{M_t}{M}\right)^\beta \exp\left(\frac{M_t - M}{M_{cm}}\right) \quad (\text{S2})$$

where M_{cm} represents the upper corner seismic moment and β represents the slope in distribution. Isolating, in brackets, the constants inside the CDF, we obtain:

$$F(M) = 1 - \left[M_t^\beta \exp\left(\frac{M_t}{M_{cm}}\right)\right] M^{-\beta} \exp\left(\frac{-M}{M_{cm}}\right) \quad (\text{S3})$$

The derivative to be calculated is a product of two functions $H(M)$ and $G(M)$:

$$H(M) = M^{-\beta} \quad (\text{S4})$$

$$G(M) = \exp\left(\frac{-M}{M_{cm}}\right) \quad (\text{S5})$$

and the derivatives are:

$$h(M) = \frac{dH(M)}{dM} = -\beta M^{-\beta-1} = -\beta \frac{1}{M^{\beta+1}} \quad (\text{S6})$$

$$g(M) = \frac{dG(M)}{dM} = -\frac{1}{M_{cm}} \exp\left(\frac{-M}{M_{cm}}\right) \quad (\text{S7})$$

The derivative of the product between two functions is:

$$\begin{aligned} \frac{d(H(M)G(M))}{dM} &= h(M)G(M) + H(M)g(M) = \\ &= -\left[\beta \frac{1}{M^{\beta+1}} \exp\left(\frac{-M}{M_{cm}}\right) + M^{-\beta} \frac{1}{M_{cm}} \exp\left(\frac{-M}{M_{cm}}\right)\right] \end{aligned} \quad (\text{S8})$$

By inserting the derivative in our CDF in the PDF calculation and considering the previously highlighted constants we get:

$$\frac{dF(M)}{dM} = f(M) = \left[M_t^\beta \exp\left(\frac{M_t}{M_{cm}}\right)\right] \left[\beta \frac{1}{M^{\beta+1}} \exp\left(\frac{-M}{M_{cm}}\right) + M^{-\beta} \frac{1}{M_{cm}} \exp\left(\frac{-M}{M_{cm}}\right)\right] \quad (\text{S9})$$

which can be transcribed as (Kagan, 2002):

$$f(M) = M_t^\beta \left[\frac{\beta}{M^\beta M} + \frac{1}{M^\beta M_{cm}} \right] \exp\left(\frac{M_t - M}{M_{cm}}\right) = \left[\frac{\beta}{M} + \frac{1}{M_{cm}} \right] \left(\frac{M_t}{M}\right)^\beta \exp\left(\frac{M_t - M}{M_{cm}}\right) \quad (\text{S10})$$

The integral after the PDF calculation becomes:

$$\int_{M_t}^{inf} M \left\{ \left[\frac{\beta}{M} + \frac{1}{M_{cm}} \right] \left(\frac{M_t}{M}\right)^\beta \exp\left(\frac{M_t - M}{M_{cm}}\right) \right\} dM \quad (\text{S11})$$

In the following equation, we move the M to the denominator of the fraction $\left(\frac{M_t}{M}\right)^\beta$ and we isolate the constant terms in the bracket:

$$\begin{aligned} & \int_{M_t}^{inf} \left[\frac{\beta}{M} + \frac{1}{M_{cm}} \right] \frac{M_t^\beta}{M^{\beta-1}} \exp\left(\frac{M_t - M}{M_{cm}}\right) dM = \\ & M_t^\beta \exp\left(\frac{M_t}{M_{cm}}\right) \int_{M_t}^{inf} \left[\frac{\beta}{M} + \frac{1}{M_{cm}} \right] \frac{1}{M^{\beta-1}} \exp\left(\frac{-M}{M_{cm}}\right) dM \end{aligned} \quad (\text{S12})$$

Now we separate the sum into two distinct integrals and place the constant part equal to K:

$$\begin{aligned} & = K \left[\int_{M_t}^{inf} \frac{\beta}{M^\beta} \exp\left(\frac{-M}{M_{cm}}\right) dM + \int_{M_t}^{inf} \frac{1}{M_{cm}} \frac{1}{M^{\beta-1}} \exp\left(\frac{-M}{M_{cm}}\right) dM \right] = \\ & K \left[\beta \int_{M_t}^{inf} M^{-\beta} \exp\left(\frac{-M}{M_{cm}}\right) dM + \frac{1}{M_{cm}} \int_{M_t}^{inf} M^{1-\beta} \exp\left(\frac{-M}{M_{cm}}\right) dM \right] \end{aligned} \quad (\text{S13})$$

We carry out a change of variables obtaining:

$$\frac{M}{M_{cm}} = X; M = XM_{cm}; dM = M_{cm}dX \quad (\text{S14})$$

Changing the variable also changes the lower limit of the integral.

If before M varied from M_t to infinity, now with $X = M / M_{cm}$ the limits of the integral range from M_t / M_{cm} to infinity and we get:

$$\begin{aligned}
& K \left[\beta \int_{M_t/M_{cm}}^{inf} (XM_{cm})^{-\beta} \exp(-X) M_{cm} dX + \frac{1}{M_{cm}} \int_{M_t/M_{cm}}^{inf} (XM_{cm})^{1-\beta} \exp(-X) M_{cm} dX \right] = \\
& K \left[\beta M_{cm}^{1-\beta} \int_{M_t/M_{cm}}^{inf} X^{-\beta} \exp(-X) dX + M_{cm}^{1-\beta} \int_{M_t/M_{cm}}^{inf} X^{1-\beta} \exp(-X) dX \right] = \\
& KM_{cm}^{1-\beta} \left[\beta \int_{M_t/M_{cm}}^{inf} X^{-\beta} \exp(-X) dX + \int_{M_t/M_{cm}}^{inf} X^{1-\beta} \exp(-X) dX \right]
\end{aligned} \tag{S15}$$

Where K is:

$$\frac{M_t^\beta}{M_{cm}^{\beta-1}} \exp\left(\frac{M_t}{M_{cm}}\right) \left[\beta \int_{M_t/M_{cm}}^{inf} X^{-\beta} \exp(-X) dX + \int_{M_t/M_{cm}}^{inf} X^{1-\beta} \exp(-X) dX \right] \tag{S16}$$

The two integrals are in the form $x^{-n}\exp(-x)$ and can be solved with the "upper" gamma incomplete functions.

From this information, we obtain the following result:

$$\frac{M_t^\beta}{M_{cm}^{\beta-1}} \exp\left(\frac{M_t}{M_{cm}}\right) \{ \beta [-\Gamma(1 - \beta, X)] + [-\Gamma(2 - \beta, X)] \} \tag{S17}$$

Returning the variable $X=M/M_{cm}$ and re-transforming the integration terms from M_t to infinity, the two incomplete gamma functions must be calculated for both $M= M_t$ and $M=\infty$.

In the resolution of the incomplete gamma function, if the second term is infinite, the result is zero. This observation gives the following result:

$$\frac{M_t^\beta}{M_{cm}^{\beta-1}} \exp\left(\frac{M_t}{M_{cm}}\right) \left\{ \beta \left[\Gamma\left(1 - \beta, \frac{M_t}{M_{cm}}\right) \right] + \left[\Gamma\left(2 - \beta, \frac{M_t}{M_{cm}}\right) \right] \right\} \tag{S18}$$

An incomplete gamma function property is the recurrence relation with which the second term inside the brackets can be explained as:

$$\text{generic function: } \Gamma(s + 1, x) = s \Gamma(s, x) + x^s e^{-x}$$

$$\text{our case: } \Gamma\left(2 - \beta, \frac{M_t}{M_c}\right) = \Gamma\left(1 - \beta + 1, \frac{M_t}{M_c}\right) =$$

Replacing this change in the previous formula we obtain:

$$\begin{aligned}
& \frac{M_t^\beta}{M_{cm}^{\beta-1}} \exp\left(\frac{M_t}{M_{cm}}\right) \left\{ \beta \left[\Gamma\left(1 - \beta, \frac{M_t}{M_{cm}}\right) \right] + \left[(1 - \beta) \Gamma\left(1 - \beta, \frac{M_t}{M_{cm}}\right) + \left(\frac{M_t}{M_{cm}}\right)^{1-\beta} \exp\left(-\frac{M_t}{M_{cm}}\right) \right] \right\} = \\
& = \frac{M_t^\beta}{M_{cm}^{\beta-1}} \exp\left(\frac{M_t}{M_{cm}}\right) \left\{ \beta \left[\Gamma\left(1 - \beta, \frac{M_t}{M_{cm}}\right) \right] + \Gamma\left(1 - \beta, \frac{M_t}{M_{cm}}\right) - \beta \left[\Gamma\left(1 - \beta, \frac{M_t}{M_{cm}}\right) \right] \right. \\
& \quad \left. + \left(\frac{M_t}{M_{cm}}\right)^{1-\beta} \exp\left(-\frac{M_t}{M_{cm}}\right) \right\} = \\
& = \frac{M_t^\beta}{M_{cm}^{\beta-1}} \exp\left(\frac{M_t}{M_{cm}}\right) \left\{ \Gamma\left(1 - \beta, \frac{M_t}{M_{cm}}\right) + \left(\frac{M_t}{M_{cm}}\right)^{1-\beta} \exp\left(-\frac{M_t}{M_{cm}}\right) \right\} = \\
& = \frac{M_t^\beta}{M_{cm}^{\beta-1}} \left(\frac{M_t}{M_{cm}}\right)^{1-\beta} \exp\left(\frac{M_t}{M_{cm}}\right) \exp\left(-\frac{M_t}{M_{cm}}\right) + \frac{M_t^\beta}{M_{cm}^{\beta-1}} \exp\left(\frac{M_t}{M_{cm}}\right) \Gamma\left(1 - \beta, \frac{M_t}{M_{cm}}\right) = \\
& \quad M_t + \frac{M_t^\beta}{M_{cm}^{\beta-1}} \exp\left(\frac{M_t}{M_{cm}}\right) \Gamma\left(1 - \beta, \frac{M_t}{M_{cm}}\right)
\end{aligned} \tag{S19}$$

To summarize, we have determined that the PDF of the tapered G - R is:

$$\left[\frac{\beta}{M} + \frac{1}{M_{cm}} \right] \left(\frac{M_t}{M}\right)^\beta \exp\left(\frac{M_t - M}{M_{cm}}\right) \tag{S20}$$

and the integral resolution (S1) is (Kagan, 2002):

$$M_t + \frac{M_t^\beta}{M_{cm}^{\beta-1}} \exp\left(\frac{M_t}{M_{cm}}\right) \Gamma\left(1 - \beta, \frac{M_t}{M_{cm}}\right) \tag{S21}$$

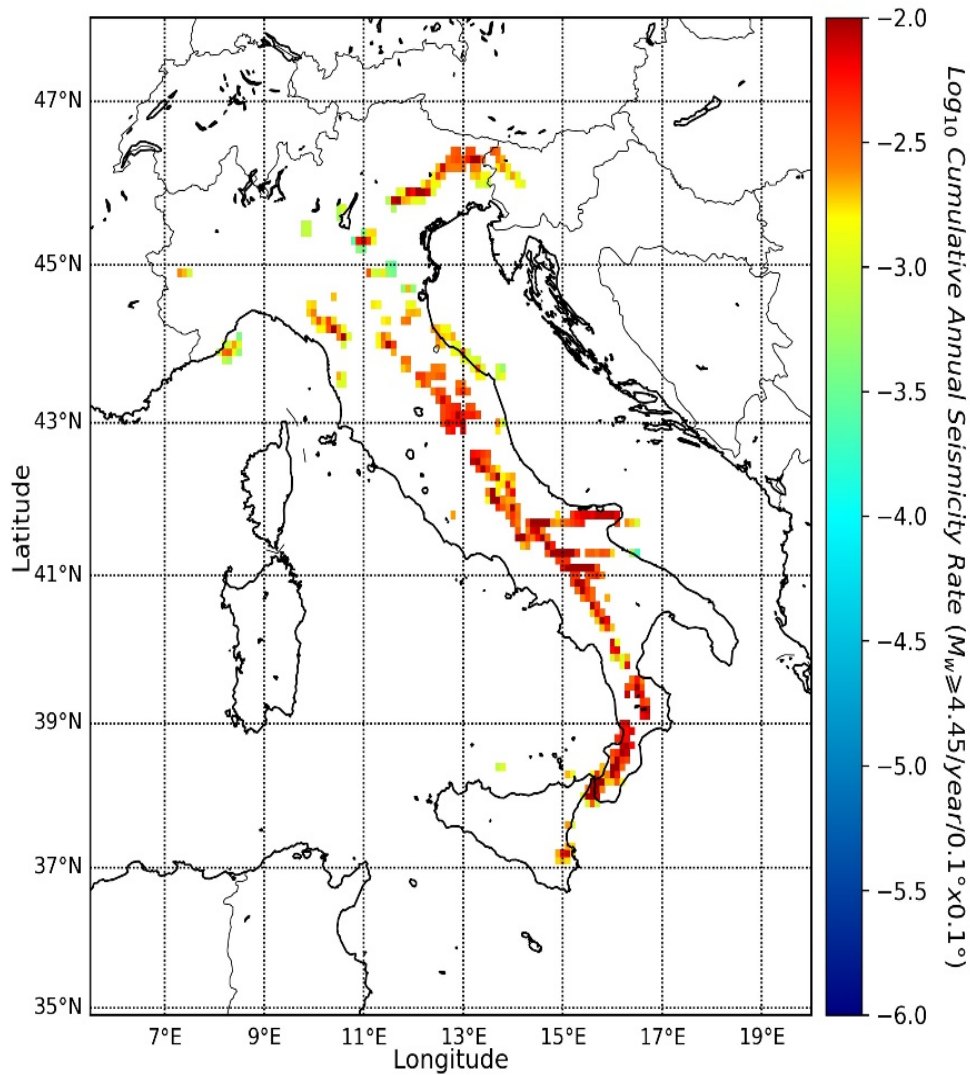


Figure S4. Results of the model obtained using only the contribution of the seismogenic sources. The *CAT_S* catalog was considered to estimate the *b*-value and the corner magnitude of the seismogenic source rate model. The color scale represents the log₁₀ of the expected cumulative annual seismicity rate ($M_w \geq 4.45$) in each cell of $0.1^\circ \times 0.1^\circ$.

S5. Ensemble Models

For the future Italian Seismic Hazard Map, we have developed six versions of a time-independent model. In this section, we report the results related to the three versions that consider the Statistical Analysis of the Completeness (SAC), i.e. the contribution of 30% (seismogenic source rate) and 70% (seismicity rate) (referred to as Ensemble 4 Model), 70% (seismogenic source rate) and 30% (seismicity rate) (referred to as Ensemble 5 Model), and 50% (seismogenic source rate) and 50% (seismicity rate) (referred to as Ensemble 6 Model). Figs. S5 and S6 show the Ensemble 6 Model, in a logarithmic and linear scale, respectively.

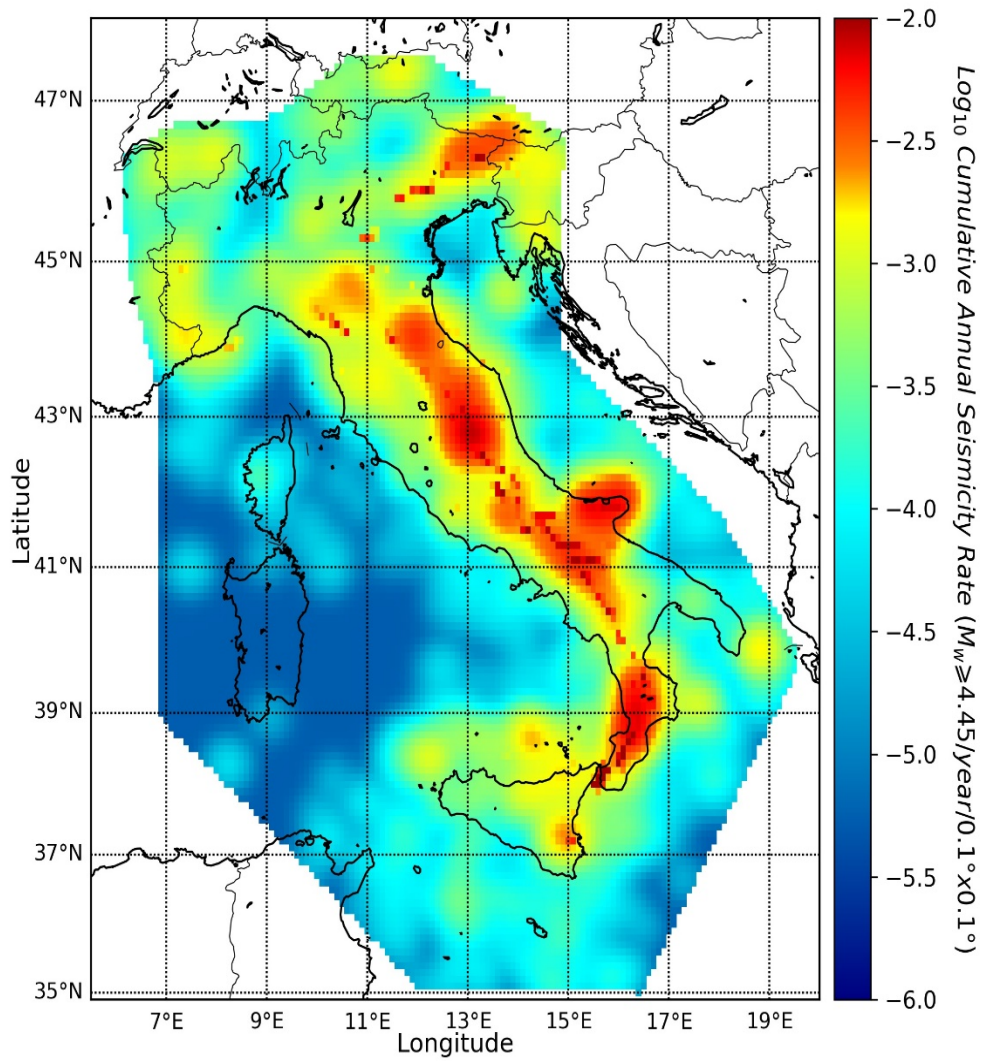


Figure S5. Results of the Ensemble model obtained from the contribution of 50% (seismogenic source rate) and 50% (seismicity rate). The *CAT_S* catalog was considered. The color scale represents the log₁₀ of the expected cumulative annual seismicity rate ($M_w \geq 4.45$) in each cell of $0.1^\circ \times 0.1^\circ$.

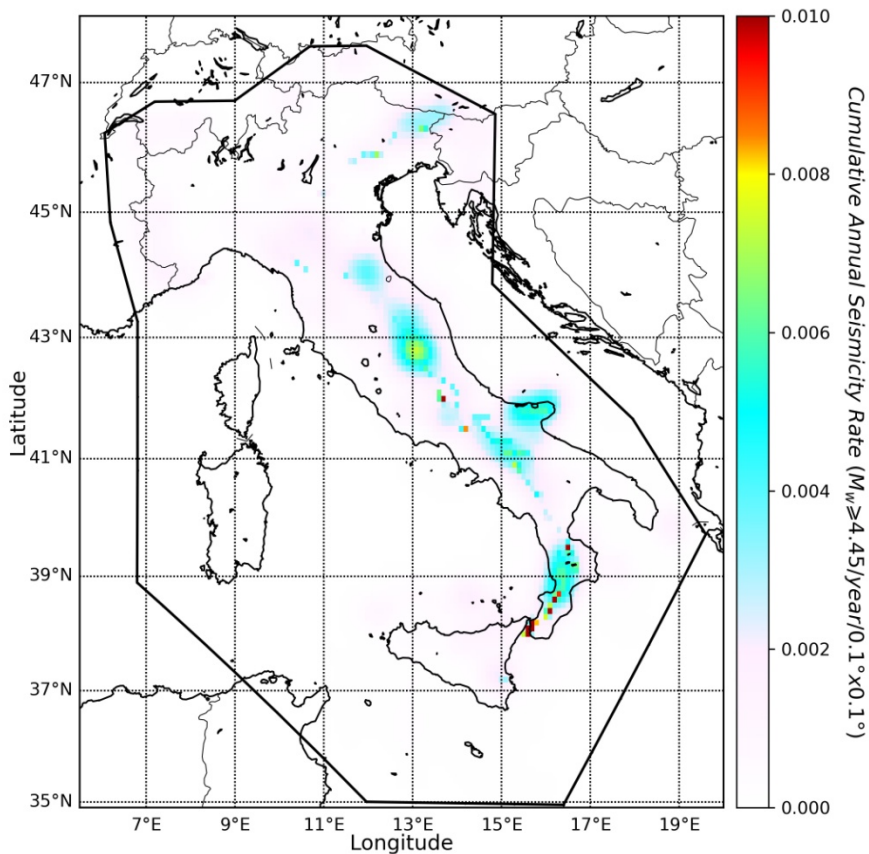


Figure S6. Results of the Ensemble model obtained from the contribution of 50% (seismogenic source rate) and 50% (seismicity rate). The *CAT_S* catalog was considered. The color scale represents the expected cumulative annual seismicity rate ($M_w \geq 4.45$ /year/ $0.1^\circ \times 0.1^\circ$).

In Fig. S7, for the “areaCPTI15”, we show the cumulative annual rates of the three ensemble models that consider the *CAT_S* catalog (Table S1b), compared with the observed seismic annual rate (1000-2017), highlighted with red dots. The logarithmic scale is used in this plot.

The plot of the three cumulative annual rate magnitude distributions of the Ensemble 4, Ensemble 5 and Ensemble 6 Models, that consider the *CAT_S* catalog, are also almost identical for all magnitudes (Fig. S7). The three ensemble models show a cumulative annual rate similar to the observed annual rate up to about 5.4, and then slightly overestimate the observed number of events for a magnitude between 5.4 and 6.2.

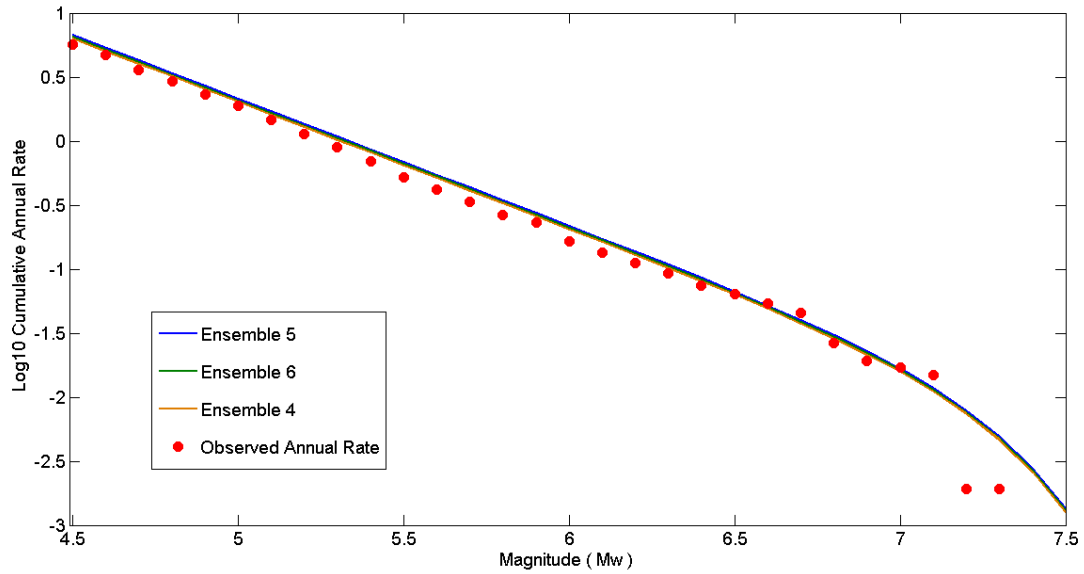


Figure S7. Expected cumulative annual rates on a logarithmic scale, for the three ensemble models that consider the *CAT_S* catalog (Ensemble 4, Ensemble 5, Ensemble 6) vs annual rate obtained from the seismicity catalog adopted in this study (CPTI15+Instrumental Catalog) (shown with red dots). The blue, brown and green lines refer to the models obtained from the contribution of 30% (seismogenic source rate) and 70% (seismicity rate), 50% (seismogenic source rate) and 50% (seismicity rate), 70% (seismogenic source rate) and 30% (seismicity rate), respectively.

References

Albini, P., R. Camassi, V. Castelli and M. Stucchi (2001). Miglioramento della qualità delle informazioni macrosismiche per un loro utilizzo nella valutazione della pericolosità sismica, Rapporto tecnico INGV-MI per il Servizio Sismico Nazionale, Milano, 195 pp. (Parte A, 43 pp.; Parte B, 152 pp.).

Albini, P., M. Stucchi and C. Mirto (2002). Valutazione di completezza su base storica, dei dati del catalogo sismico CPTI (1999) nell'area corrispondente alle ZS n. 5 e 6 in ZS4 (Belluno/Cansiglio e Asolo/Vittorio Veneto), Progetto GNDT "Scenari di danno in area veneto-friulana". Rapporto tecnico INGV-MI, 5 pp.

Albarello, D., R. Camassi and A. Rebez (2001). Detection of space and time heterogeneity in the completeness level of a seismic catalogue by a "robust" statistical approach: an application to the Italian area, *Bull. Seism. Soc. Am.*, 91 (6), 1694-1703.

DISS Working Group (2018). Database of Individual Seismogenic Sources (DISS), Version 3.2.1: A compilation of potential sources for earthquakes larger than M 5.5 in Italy and surrounding areas. <http://diss.rm.ingv.it/diss/>, © INGV 2018-Istituto Nazionale di Geofisica e Vulcanologia doi:10.6092/INGV.IT-DISS3.2.1.

Hiemer, S., J. Woessner, R. Basili, L. Danciu, D. Giardini and S. Wiemer (2014). A smoothed stochastic earthquake rate model considering seismicity and fault moment release for Europe, *Geophys. J. Int.*, 198, 1159-1172.

Kagan, Y.Y. (2002). Seismic moment distribution revisited: I. Statistical results, *Geophys. J. Int.*, 148, 520-541.

Meletti C., V. D'Amico, F. Martinelli and A. Rovida (2018). Stima della completezza e individuazione delle repliche del catalogo CPTI15. CPS-INGV internal report (confidential).

Rovida, A., M. Locati, R. Camassi, B. Lolli and P. Gasperini (2016). CPTI15, The 2015 Version of the Parametric Catalogue of Italian, available at: <http://doi.org/10.6092/INGV.IT-CPTI15>.